Scalable Algorithms for Implicit Fluid Plasma Simulation

L. Chacón

Los Alamos National Laboratory

P.O. Box 1663, Los Alamos, NM 87545

LANL collaborators: A. Stanier

SNL collaborators: J. N. Shadid, R. Pawlowski, E. Cyr, R. Tuminaro, P. Lin

Funding: DOE-ASCR AMR program, DOE-FES Basic Plasma Physics program, SCIDAC

BOUT++ Workshop

Livermore, CA

August 14-17, 2018

Outline

- Motivation: extended (two-fluid) MHD and the tyranny of scales
- Parabolization of XMHD: key for SCALABILITY
- 2D Low-β extended MHD (large guide field)
  - Application to magnetic reconnection
- 3D extended MHD solvers

"The tyranny of scales"

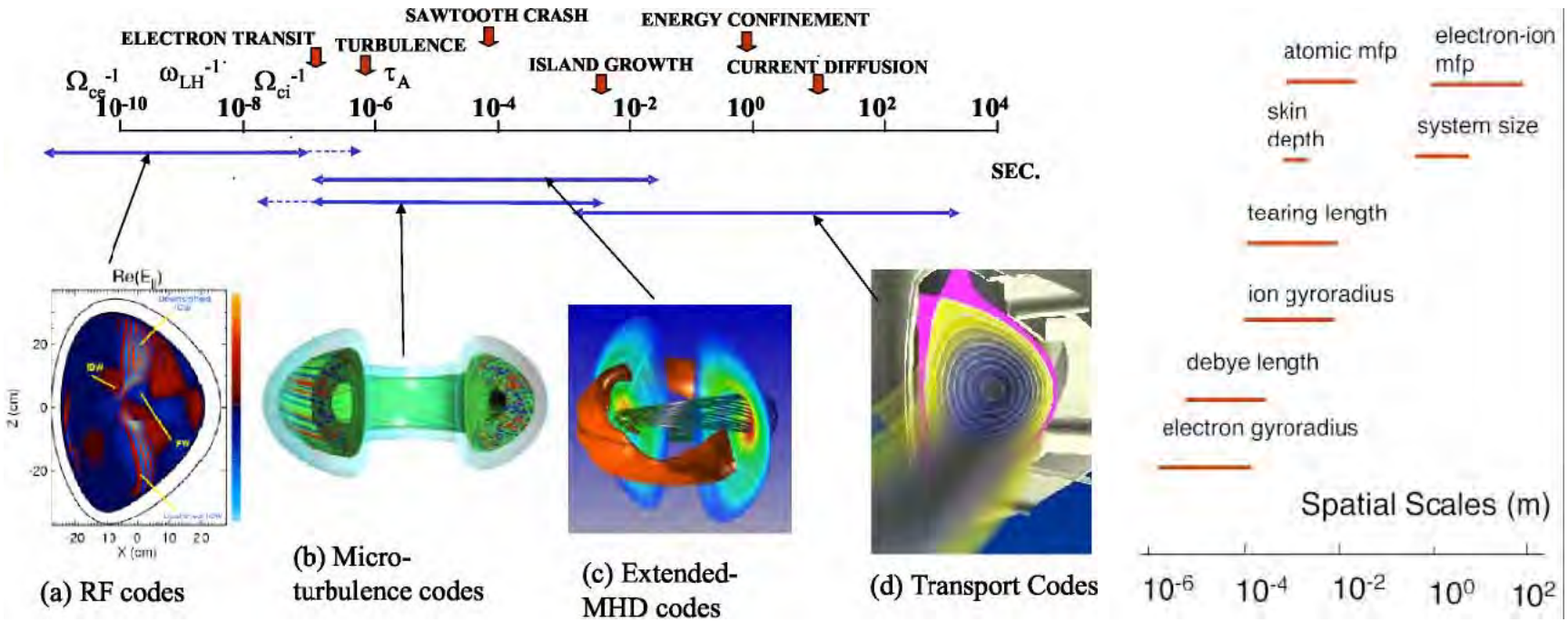

Luis Chacon, chacon@lanl.gov

Algorithmic challenges in XMHD

- XMHD has mixed character, with strongly hyperbolic and parabolic components.
- Numerically, XMHD is a nonlinear algebraic system of very stiff equations:
  - Parabolic stiffness (diffusion): $\kappa(J) \sim \frac{\Delta t\, D}{\Delta x^2} \gg 1$
  - Hyperbolic stiffness (linear and dispersive waves): $\kappa(J) \sim \Delta t\, \omega_{fast} \sim \frac{\Delta t}{\Delta t_{CFL}} \gg 1$
- Brute-force algorithms will not be able to cover the span between disparate time/length scales, regardless of computer power.
- Key algorithmic requirement: SCALABILITY $[CPU \sim \mathcal{O}(N/n_p)]$!
  - Minimize number of degrees of freedom N: spatial adaptivity.
  - Follow slowest time scales (application dependent): implicit time stepping.
- Scalable implicit methods require MULTILEVEL approaches:

$$CPU \sim \mathcal{O}\left(\frac{N\,\log(N)}{n_p^{\beta}}\right)\ ,\ \beta \lesssim 1$$

Luis Chacon, chacon@lanl.gov

Implicit time-stepping: Jacobian-Free Newton-Krylov Methods

- Objective: solve nonlinear system $\vec{G}(\vec{x}^{n+1}) = \vec{0}$ efficiently (scalably).
- Converge nonlinear couplings using Newton-Raphson method: $\left.\frac{\partial \vec{G}}{\partial \vec{x}}\right|_k \delta\vec{x}_k = -\vec{G}(\vec{x}_k)$.
- Jacobian-free implementation: $\left(\frac{\partial \vec{G}}{\partial \vec{x}}\right)_k \vec{y} = J_k \vec{y} = \lim_{\epsilon \to 0} \frac{\vec{G}(\vec{x}_k + \epsilon\vec{y}) - \vec{G}(\vec{x}_k)}{\epsilon}$
- Krylov method of choice: GMRES (nonsymmetric systems).
- Right preconditioning: solve equivalent Jacobian system for $\delta y = P_k \delta\vec{x}$:

$$J_k P_k^{-1} \underbrace{P_k \delta\vec{x}}_{\delta\vec{y}} = -\vec{G}_k$$

> Approximations in preconditioner do not affect accuracy of converged solution; they only affect efficiency!

- The rest of the talk will discuss the development of suitable preconditioners P_k!

Luis Chacon, chacon@lanl.gov

Preconditioning: multilevel (multigrid) methods

- MG employs a divide-and-conquer approach to attack error components in the solution.
  - Oscillatory components of the error are "EASY" to deal with (if a SMOOTHER exists)
  - Smooth components are DIFFICULT.

Idea: Coarsen grid to make "smooth" components oscillatory, and proceed recursively

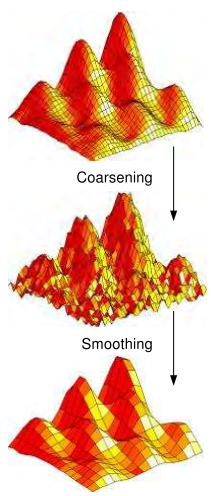

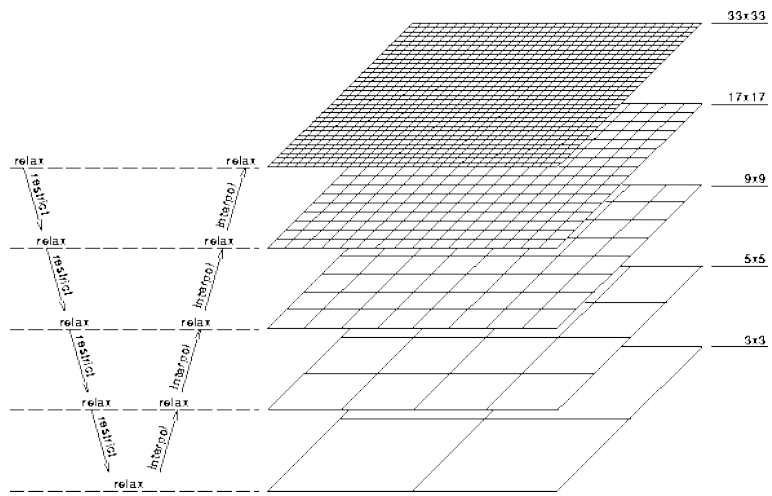

- SMOOTHER is make or break of MG!
- Stiff hyperbolic equations challenge MG, because smoothers are hard to formulate.
- In general, smoothers are easy to find for parabolic systems: PARABOLIZATION!

Luis Chacon, chacon@lanl.gov

MG methods for stiff hyperbolic equations: Parabolization and block factorization (Schur complement)

- Parabolization is a natural consequence of implicit timestepping:

$$\partial_t u = \frac{1}{\epsilon}\partial_x v \ , \ \partial_t v = \frac{1}{\epsilon}\partial_x u.$$

$$u^{n+1} = u^n + \frac{\Delta t}{\epsilon}\partial_x v^{n+1}, v^{n+1} = v^n + \frac{\Delta t}{\epsilon}\partial_x u^{n+1}.$$

$$\boxed{\left[I - \left(\frac{\Delta t}{\epsilon}\right)^2 \partial_{xx}\right] u^{n+1} = u^n + \frac{\Delta t}{\epsilon}\partial_x v^n}$$

- This can be exploited to develop optimal MG solvers for stiff hyperbolic systems
- PARABOLIZATION via BLOCK FACTORIZATION (Schur complement):

$$\begin{bmatrix} D_1 & U \\ L & D_2 \end{bmatrix} = \begin{bmatrix} I & UD_2^{-1} \\ 0 & I \end{bmatrix} \begin{bmatrix} D_1 - UD_2^{-1}L & 0 \\ 0 & D_2 \end{bmatrix} \begin{bmatrix} I & 0 \\ D_2^{-1}L & I \end{bmatrix}.$$

$$D_1 - UD_2^{-1}L = \left[I - \left(\frac{\Delta t}{\epsilon}\right)^2 \partial_{xx}\right]$$

Luis Chacon, chacon@lanl.gov

Our approach to a successful fully implicit algorithm for XMHD

- Fully implicit time-stepping: JFNK + MG
- Combination of Krylov methods and MG preconditioning is optimal:
  - Even if a smoother exists, MG is remarkably temperamental
  - MG preconditioning provides scalability
  - Krylov solver provides robustness
- Exploit parabolization of hyperbolic eqs for effective MG
- We have successfully applied this recipe to various MHD systems:
  - 2D reduced resistive[1] and Hall MHD[2] (high-β)
  - 3D resistive[3] and Hall MHD[4]
- We bring along a new application, 2D low-β extended MHD[5], and revisit our 3D extended MHD work.

[1] LC, D. A. Knoll, J. M. Finn, J. Comput. Phys., 178, 15-36 (2002)
[2] LC, D. A. Knoll, J. Comput. Phys., 188 (2), 573-592 (2003)
[3] LC, Phys. Plasmas 15, 056103 (2008)
[4] LC, J. Physics: Conf. Series, 125, 012041 (2008); JCP, in preparation
[5] LC and A. Stanier, J. Comput. Phys, 326 (2016)

Luis Chacon, chacon@lanl.gov

2D low-β extended MHD

LC and A. Stanier, J. Comput. Phys, 326 (2016)

Los Alamos NATIONAL LABORATORY EST. 1943

Luis Chacon, chacon@lanl.gov

Extended (two-fluid, Hall) MHD model equations

$$
\begin{aligned}
\frac{\partial \rho}{\partial t} &+ \nabla \cdot (\rho \vec{v}) = 0, \\
\frac{\partial \vec{B}}{\partial t} &+ \nabla \times \vec{E} = 0, \\
\frac{\partial (\rho \vec{v})}{\partial t} + \nabla \cdot \left[\rho \vec{v}\vec{v} - \vec{B}\vec{B} \right. &+ \left. \overleftrightarrow{\Pi} + \overleftrightarrow{I}(p + \frac{B^2}{2}) \right] = 0, \\
\frac{\partial p_e}{\partial t} + \nabla \cdot (\vec{v} p_e) &+ (\gamma - 1) p_e \nabla \cdot \vec{v} = (\gamma - 1)(S - \nabla \cdot \vec{q}).
\end{aligned}
$$

$$\vec{v} = \frac{m_i \vec{v}_i + m_e \vec{v}_e}{m_i + m_e} \approx \vec{v}_i \ ; \ \vec{v}_e = \vec{v}_i - d_i \frac{\vec{j}}{\rho}$$

$$\text{Ohm's Law} : \vec{E} = -\vec{v} \times \vec{B} + \eta \vec{j} - \frac{d_i}{\rho}(\vec{j} \times \vec{B} - \nabla p_e - \nabla \cdot \overleftrightarrow{\Pi}_e) - \frac{d_e^2}{d_i} \frac{d\vec{v}_e}{dt}$$

Luis Chacon, chacon@lanl.gov

Low-β extended MHD limit

- Large guide field regime $B_z \gg B_p$, $\beta = 2\mu_0 p/B_0 \ll 1$ (tokamak, solar corona, etc.)
- Cold ions ($T_i \ll T_e$), to neglect finite Larmor radius effects (gyroviscosity)

$$
\begin{aligned}
\partial_t F + \mathbf{v}_s \cdot \nabla F &= \eta \nabla^2 \psi - \eta_H \nabla^4 \psi, \\
\partial_t \Omega + \mathbf{v} \cdot \nabla \Omega &= \mathbf{B} \cdot \nabla J + \mu \nabla^2 \Omega \\
F = \psi - d_e^2 J \quad &; \quad J = \nabla^2 \psi \; ; \; \Omega = \nabla^2 \phi \\
\mathbf{v} = \mathbf{z} \times \nabla \phi \quad &; \quad \mathbf{B} = \mathbf{z} \times \nabla \psi \; ; \; \mathbf{v}_s = \mathbf{z} \times \nabla (\phi - \rho_s^2 \Omega)
\end{aligned}
$$

- Here:
  - $\rho_s = \omega_i^{-1} (T_e/m_i)^{1/2}$ is the sound Larmor radius
  - $d_e = c/\omega_{pe}$ is electron skin depth (measure of importance of inertial effects)
- We choose to transform vorticity equation in terms of streamfunction (requires Poisson inversion in residual; critical for large-scale performance with 2nd-order discretizations):

$$
\partial_t \phi + \nabla^{-2} \left[\mathbf{v} \cdot \nabla (\nabla^2 \phi) - \mathbf{B} \cdot \nabla (\nabla^2 \Psi) \right] = \mu \nabla^2 \phi
$$

Luis Chacon, chacon@lanl.gov

Low-β extended MHD system: properties and challenges

- The low-β extended MHD model looks deceptively simple:
  - Supports two microscopic length scales, ρ_s and d_e
  - Supports multiple time scales (dispersive waves):

$$\omega^2 = k_\parallel^2 \frac{1+\rho_s^2 k^2}{1+d_e^2 k^2}$$

  - Fast dispersive waves supported for $\rho_s > d_e$ [or $\beta > (m_e/m_i)^2$]:

$$\omega \approx \begin{cases} \pm k_\parallel, & k\rho_s < 1 \,(\text{Alfven wave}) \\ \pm \rho_s k_\parallel k, & k\rho_s > 1 > k d_e \,(\text{Kinetic Alfven wave; quadratic}) \\ \pm \frac{\rho_s}{d_e} k_\parallel, & k d_e > 1 \,(\text{Scaled Alfven wave}) \end{cases}$$

- There currently exists no scalable solver for this system, and practitioners revert to direct or ILU solvers/smoothers to deal with it.[6,7]

[6] K. Germaschewski et al., NUMERICAL MODELING OF SPACE PLASMA FLOWS, ASP Conference Series, Vol. 359, 2006
[7] S. Ovtchinnikov et al., J. Comput. Phys. 225 (2007) 1919–1936.

Physics-based preconditioning strategy

- Consider linearized equations around a given state ϕ_0, ψ_0, and Ω_0:

$$\mathcal{L}_\eta^s \tilde{\psi} - \mathbf{B}_0^* \cdot \nabla \tilde{\phi} + \rho_s^2 \mathbf{B}_0 \cdot \nabla \tilde{\Omega} = -\mathbf{G}_\psi, \quad (1)$$

$$\mathcal{L}_\mu \tilde{\Omega} + \tilde{\mathbf{v}} \cdot \nabla \Omega_0 - \mathbf{B}_0 \cdot \nabla (\nabla^2 \tilde{\psi}) + (\mathbf{z} \times \nabla J_0) \cdot \nabla \tilde{\psi} = -\nabla^2 \mathbf{G}_\phi, \quad (2)$$

$$\mathcal{L}_\eta^s = \frac{\mathbb{I} - d_e^2 \nabla^2}{\Delta t} + \mathbf{v}_{s,0} \cdot \nabla - d_e^2 (\mathbf{v}_0 \cdot \nabla) \nabla^2 - \eta \nabla^2 + \eta_H \nabla^4,$$

$$\mathcal{L}_\mu = \frac{\mathbb{I}}{\Delta t} + \mathbf{v}_0 \cdot \nabla - \mu \nabla^2.$$

- First key step: commute (approximately) the Laplacian operator in vorticity equation:[8]

$$\mathcal{L}_\mu \tilde{\phi} - \mathbf{B}_0 \cdot \nabla \tilde{\psi} \approx -\mathbf{G}_\phi. \quad (3)$$

[8] LC, Knoll, Finn, JCP 2002

Physics-based preconditioning strategy (cont.)

- Replace this equation into flux equation, to find:

$$\left[\frac{\mathbb{I} - d_e^2\nabla^2}{\Delta t} + \mathbf{v}_{s,0}\cdot\nabla - d_e^2(\mathbf{v}_0\cdot\nabla)\nabla^2 + \eta_H\nabla^4\right]\tilde{\psi} \qquad \text{(Advection, Diffusion, Inertia)}$$

$$-(\mathbf{B}_0^*\cdot\nabla)\boxed{\mathcal{L}_\mu^{-1}}(\mathbf{B}_0\cdot\nabla)\tilde{\psi} \qquad \text{(Alfven wave)}$$

$$-(\mathbf{B}_0\cdot\nabla)\boxed{\mathcal{L}_\mu^{-1}}(\mathbf{B}_0^\dagger\cdot\nabla)\tilde{\psi}$$

$$+\rho_s^2(\mathbf{B}_0\cdot\nabla)\boxed{\mathcal{L}_\mu^{-1}}(\mathbf{B}_0\cdot\nabla)\nabla^2\tilde{\psi} \qquad \text{(KAW wave)}$$

$$= \quad -\mathbf{G}_\psi + (\mathbf{B}_0^*\cdot\nabla)\mathcal{L}_\mu^{-1}\left[-\mathbf{G}_\phi - \rho_s^2(-\nabla^2\mathbf{G}_\phi)\right]$$

where:

$$\mathbf{B}_0^* = \mathbf{z}\times\nabla F_0 \quad ; \quad \mathbf{B}_0^\dagger = \rho_s^2\mathbf{z}\times\nabla J_0.$$

Physics-based preconditioning strategy (cont.)

- As written, however, this equation is impractical to solve due to the presence of $\mathcal{L}_\mu^{-1}$ operators.
- Postulate a stationary iterative procedure:[9] $\mathcal{L}_\mu = \mathcal{D}_\mu - (\mathcal{D}_\mu - \mathcal{L}_\mu)$
- Lagging the off-diagonal component gives:

$$\begin{aligned} \tilde{\phi}^{m+1} &= \mathcal{D}_\mu^{-1}\mathbf{B}_0 \cdot \nabla\tilde{\psi}^{m+1} + \mathrm{rhs}_\phi^m, \qquad (4) \\ \tilde{\Omega}^{m+1} &= \mathcal{D}_\mu^{-1}\left[\mathbf{B}_0 \cdot \nabla(\nabla^2\tilde{\psi}^{m+1}) + \tilde{\mathbf{B}}^{m+1} \cdot \nabla(\nabla^2\psi_0)\right] + \mathrm{rhs}_\Omega^m. \end{aligned}$$

- Replacing these results into the flux equation finally gives a tractable equation for $\tilde{\psi}$:

$$\begin{aligned} \mathcal{L}_\eta^s\tilde{\psi}^{m+1} &- (\mathbf{B}_0 \cdot \nabla)\mathcal{D}_\mu^{-1}(\mathbf{B}_0 \cdot \nabla)\tilde{\psi}^{m+1} \qquad (5) \\ &+ \rho_s^2(\mathbf{B}_0 \cdot \nabla)\mathcal{D}_\mu^{-1}\left[(\mathbf{B}_0 \cdot \nabla)\nabla^2\tilde{\psi}^{m+1} + (\mathbf{z} \times \nabla J_0) \cdot \nabla\tilde{\psi}^{m+1}\right] \qquad (6) \\ &= -\mathbf{G}_\psi + (\mathbf{B}_0 \cdot \nabla)\left[\mathrm{rhs}_\phi^m - \rho_s^2\mathrm{rhs}_\Omega^m\right]. \qquad (7) \end{aligned}$$

[9] LC, Knoll, Finn, JCP 2002

Physics-based preconditioning strategy (cont.)

- Summary of preconditioning strategy:
  - Solve for RHS, $\nabla^{-2}[-\mathbf{G}_\Omega - \mathcal{L}_\mu(-\mathbf{G}_\phi)] \equiv \mathrm{rhs}_\phi$
  - Perform a few iterations ($m \lesssim 2$) on parabolized scalar equation:

$$
\begin{aligned}
\mathcal{L}_\eta^s \tilde{\psi}^{m+1} \quad &- \quad (\mathbf{B}_0 \cdot \nabla)\mathcal{D}_\mu^{-1}(\mathbf{B}_0 \cdot \nabla)\tilde{\psi}^{m+1} \\
&+ \quad \rho_s^2(\mathbf{B}_0 \cdot \nabla)\mathcal{D}_\mu^{-1}\left[(\mathbf{B}_0 \cdot \nabla)\nabla^2\tilde{\psi}^{m+1} + (\mathbf{z} \times \nabla J_0) \cdot \nabla\tilde{\psi}^{m+1}\right] \\
&= \quad -\mathbf{G}_\psi + (\mathbf{B}_0 \cdot \nabla)\left[\mathrm{rhs}_\phi^m - \rho_s^2 \mathrm{rhs}_\Omega^m\right].
\end{aligned}
$$

  - Update vorticity and streamfunction:

$$
\begin{aligned}
\mathcal{L}_\mu\tilde{\Omega} + \tilde{\mathbf{v}} \cdot \nabla\Omega_0 - \mathbf{B}_0 \cdot \nabla(\nabla^2\tilde{\psi}) + (\mathbf{z} \times \nabla J_0) \cdot \nabla\tilde{\psi} \quad &= \quad -\mathbf{G}_\Omega, \\
\tilde{\Omega} - \nabla^2\tilde{\phi} \quad &= \quad -\mathbf{G}_\phi.
\end{aligned}
$$

Linear verification results

- We choose the cosine **doubly periodic tearing mode** problem:[10]

$$\psi_0 = J_0 = \cos(y) \; ; \; x \in (-2\pi, 2\pi) \; ; \; y \in (-\pi, \pi)$$

- Doubly periodic domain (can be integrated in half domain using symmetry BCs)

- We choose two regimes with $k_x = \frac{2\pi}{L_x} = 0.5$:

  - $\rho_s = 0.1$, $d_e = 0.01$, , $\eta = \mu = 10^{-5}$, $\eta_H = 0$ ($\gamma = 2.5797 \times 10^{-3}$)
  - $\rho_s = 0.01$, $d_e = 0.1$, $\eta = \mu = 10^{-5}$, $\eta_H = 0$ ($\gamma = 5.2841 \times 10^{-3}$)

[10] Bhattacharjee et al, PoP 12 (2005)

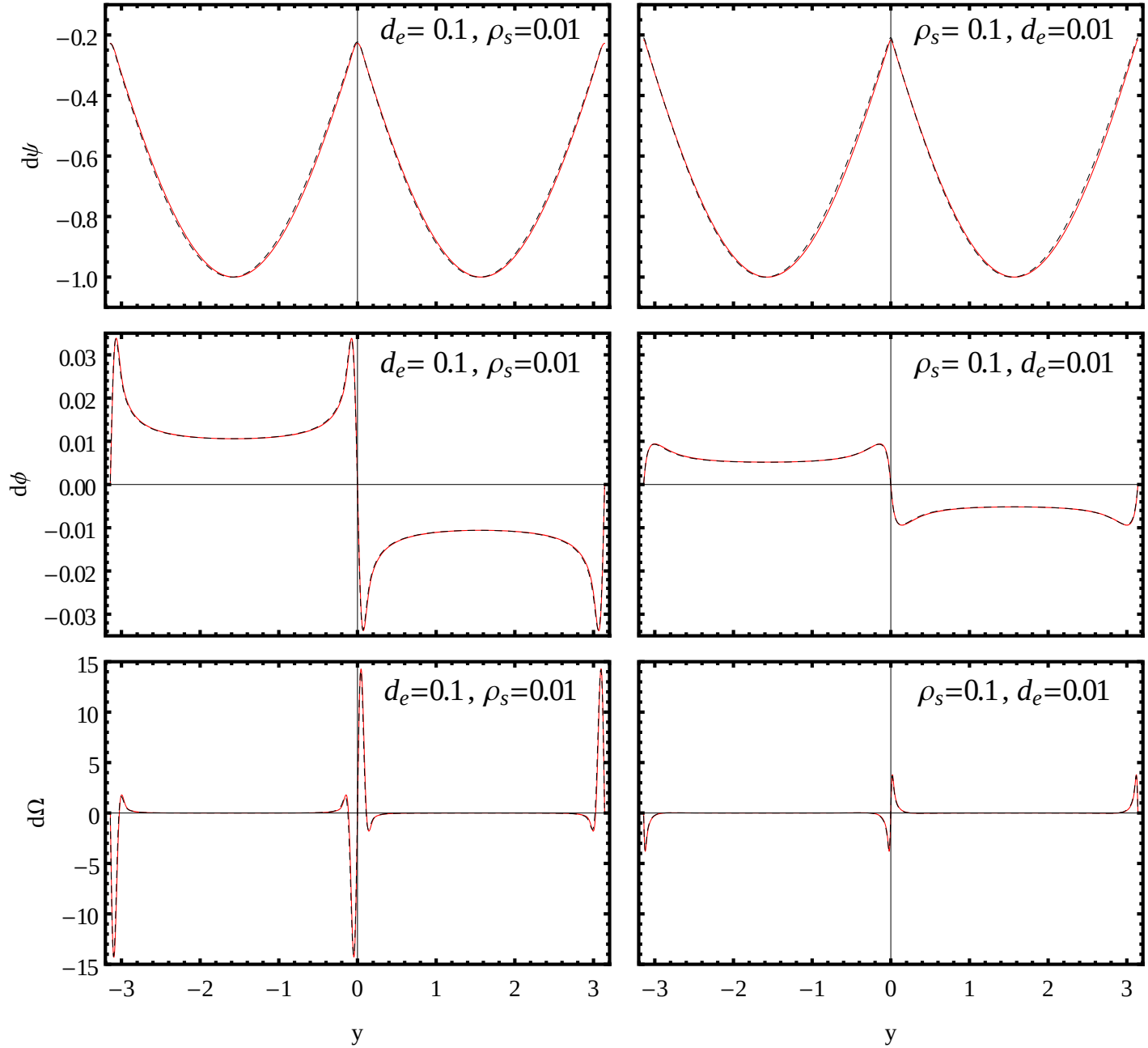

Los Alamos NATIONAL LABORATORY EST. 1943

Luis Chacon, chacon@lanl.gov

Serial grid convergence study (doubly periodic tearing mode)

$$\rho_s = 0.1, d_e = 0.01$$

100 time steps, $\Delta t = 1.0$, 2 SI iterations, 2 V(3,3) MG cycles

Grid	η_H	GMRES/Δt	Newton/Δt	WCT (s)	WCT$_{exp}$/WCT	$\Delta t/\Delta t_{exp}$
32×32	3×10^{-4}	0.0	2.0	48	1.5	10
64×64	7.7×10^{-5}	0.0	2.0	192	9.4	41.5
128×128	1.9×10^{-5}	0.2	2.4	911	32	166
256×256	4.8×10^{-6}	0.4	2.6	4280	107	664
512×512	1.2×10^{-6}	1.4	2.9	21170	392	2656

- Explicit solver is RK2
  - Each step requires inversion of elliptic couplings ($\nabla^2\phi = \Omega$ and $(1/\Delta t - d_e^2\nabla^2)\Psi = F$)
  - We solve these to same relative tolerance as implicit solve
- Implicit solver is BDF2
  - $rtol = 10^{-4}$
  - GMRES/$\Delta t < 1$ because we use preconditioner for initial guess
  - Hyperresistivity adapts to provide dissipation at grid scale (stiffness does not grow with mesh)

Luis Chacon, chacon@lanl.gov

Time-step convergence study (doubly periodic tearing mode)

$$\rho_s = 0.1, d_e = 0.01$$

64x64, $T_{max} = 100$, 2 SI iterations, 2 V(3,3) MG cycles

Δt	GMRES/Δt	Newton/Δt	WCT (s)	WCT$_{exp}$/WCT	$\Delta t/\Delta t_{exp}$
0.1	0.0	1.0	1100	1.6	4
0.5	0.0	2.0	366	5	21
1.0	0.0	2.0	192	9.4	41.5
5	1.2	4.2	92	20	207

$$\frac{WCT_{exp}}{WCT} \sim \Delta t^{0.6}$$

- It is advantageous to use larger time steps for efficiency (up to a point, determined by accuracy and/or algorithmic degradation)

Luis Chacon, chacon@lanl.gov

Parallel weak convergence study (doubly periodic tearing mode)

$$\rho_s = 0.1, d_e = 0.01$$

$\Delta t = 1.0$, 10 time steps, 2 SI iterations, 2 V(3,3) MG cycles

N_p	Grid	η_H	GMRES/Δt	Newt/Δt	WCT (s)	WCT/PC	$\frac{\text{WCT}_{\text{exp}}}{\text{WCT}}$
1	64×64	7.7×10^{-5}	0	2.8	72.3	25.8	6.4
4	128×128	1.9×10^{-5}	0	2.9	79.5	27.4	24.3
16	256×256	4.8×10^{-6}	0	3.0	91.8	30.6	95.3
64	512×512	1.2×10^{-6}	0.3	3.4	139.2	37.6	276.3
256	1024×1024	3.0×10^{-7}	1.0	3.6	188.6	41	881.9
1024	2048×2048	7.5×10^{-8}	2.1	3.7	265.3	45.7	2705
4096	4096×4096	1.9×10^{-8}	4.7	4.3	556.3	61.8	6758

$$WCT/PC \sim \log(N_p)$$

- Implicit timestep is kept constant!
- WCT increases only by factor of 8 between 1 and 4096 cores (compared to factor of 4096 for explicit from CFL constraints)

Luis Chacon, chacon@lanl.gov

Nonlinear application: Magnetic reconnection

Figure 1: NASA video of a geomagnetic substorm

- Observations confirm magnetic reconnection is explosively fast
- Theory requires magnetic field dissipation at microscopic length scales for reconnection to occur
- Dissipation in space environment is arbitrarily small, length scales arbitrarily large

Luis Chacon, chacon@lanl.gov

Nonlinear simulations: fast reconnection in low-β regimes

- We have performed 2D nonlinear simulations to understand fast reconnection in low-β regimes[11]
  - Developed a **nonlinear theory** for fast reconnection in low-β regimes.
  - **Compared against kinetic simulations (VPIC)** to understand fundamental differences between kinetic and fluid reconnection
- We conclude that reconnection is FAST (independent of dissipation and system size) for all regimes with finite d_e, ρ_s (a controversial result)

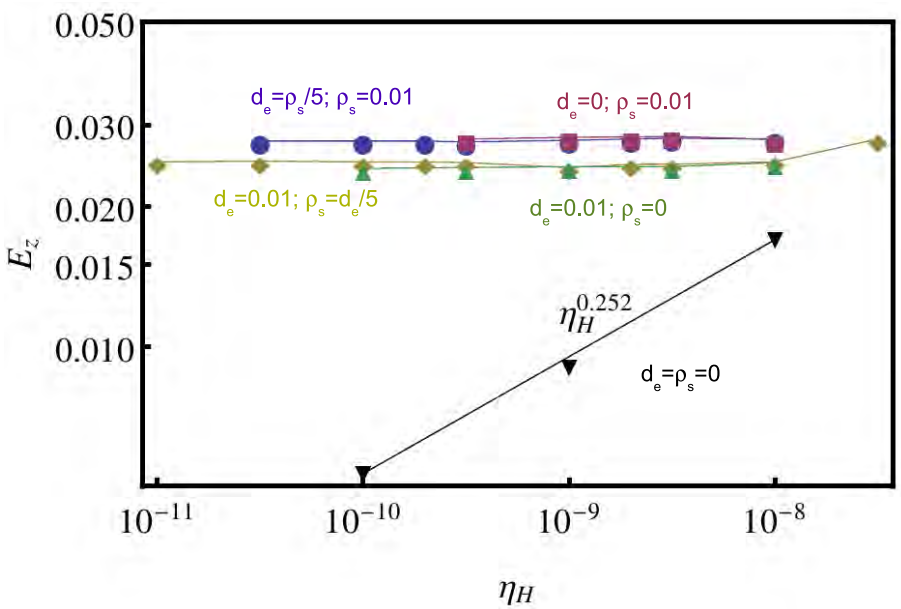

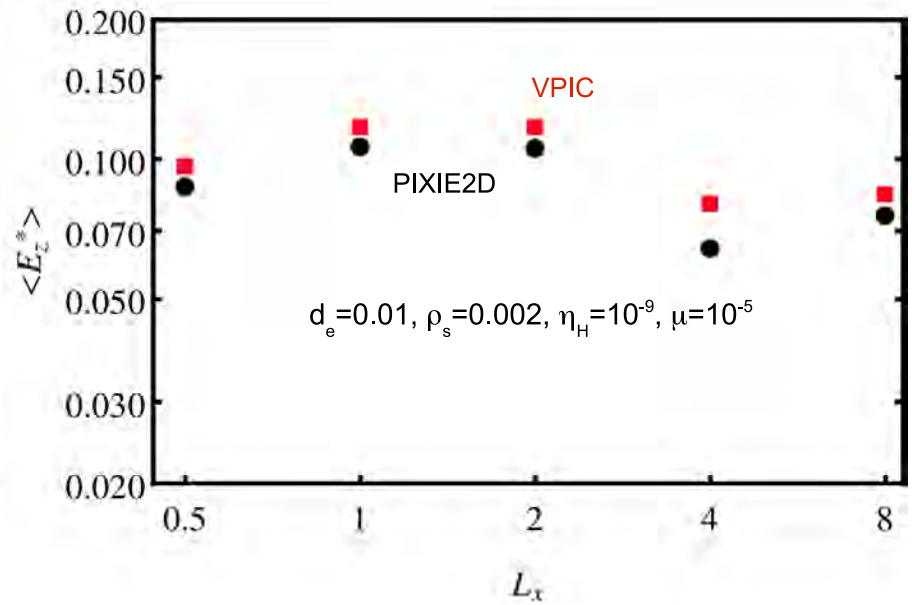

[11] Stanier et al, Phys. Plasmas, 2014, 2015

Luis Chacon, chacon@lanl.gov

Nonlinear simulations: fast reconnection in low-β regimes (cont.)

- Agreement between fluid and kinetic is good also in the reconnection time history[12]
- Harris sheet, $d_e = 0.01$, $\rho_s = 2 \times 10^{-3}$, $\eta_H = 10^{-9}$, $\mu = 10^{-5}$

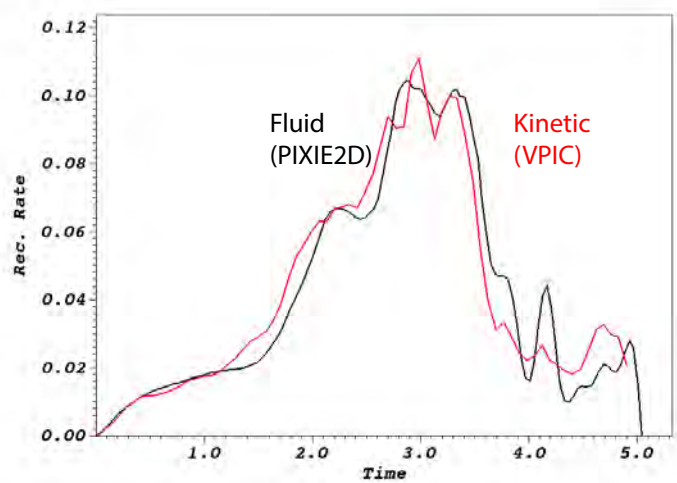

(a) $d_e = 0.01,\ \rho_s = 2 \times 10^{-3}$

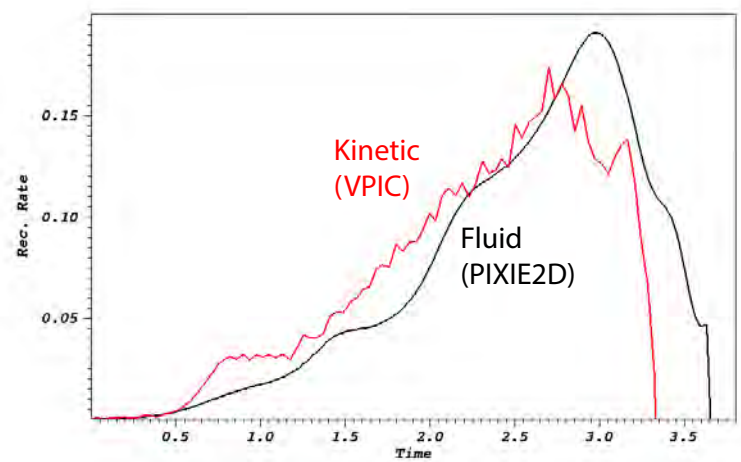

(b) $\rho_s = 0.01,\ d_e = 2 \times 10^{-3}$

[12] A. Stanier et al., Phys. Plasmas, 2014, 2015

Luis Chacon, chacon@lanl.gov

Nonlinear simulations: fast reconnection in low-β regimes (cont.)

- **Harris sheet**, $\rho_s = 2 \times 10^{-3}$, $\eta_H = 10^{-9}$, $\mu = 10^{-5}$
- Up-down symmetry is enforced in fluid simulation

(a) $de = 0.01$; $\rho_s = 0.002$

(b) $de = 0.002$; $\rho_s = 0.01$

3D *resistive* MHD implicit solver

L. Chacón, Phys. Plasmas 15, 056103 (2008)

Los Alamos NATIONAL LABORATORY EST. 1943

Luis Chacon, chacon@lanl.gov

Resistive MHD model equations

$$
\begin{aligned}
\frac{\partial \rho}{\partial t} &+ \nabla \cdot (\rho \vec{v}) = 0, \\
\frac{\partial \vec{B}}{\partial t} &+ \nabla \times \vec{E} = 0, \\
\frac{\partial (\rho \vec{v})}{\partial t} + \nabla \cdot \left[\rho \vec{v}\vec{v} - \vec{B}\vec{B} \right. &+ \left. \overleftrightarrow{\Pi} + \overleftrightarrow{I}(p + \frac{B^2}{2}) \right] = 0, \\
\frac{\partial p_e}{\partial t} + \nabla \cdot (\vec{v} p_e) &+ (\gamma - 1) p_e \nabla \cdot \vec{v} = (\gamma - 1)(S - \nabla \cdot \vec{q}).
\end{aligned}
$$

- Simple viscous closure for stress tensor: $\overleftrightarrow{\Pi} \approx -\rho \nu_i \nabla \vec{v}$
- Resistive Ohm's law:

$$\vec{E} = -\vec{v} \times \vec{B} + \eta \vec{j}$$

Luis Chacon, chacon@lanl.gov

Resistive MHD Jacobian block structure

- The linearized resistive MHD model has the following couplings:

$$
\begin{aligned}
\delta\rho &= L_\rho(\delta\rho, \delta\vec{v}) \\
\delta T &= L_T(\delta T, \delta\vec{v}) \\
\delta\vec{B} &= L_B(\delta\vec{B}, \delta\vec{v}) \\
\delta\vec{v} &= L_v(\delta\vec{v}, \delta\vec{B}, \delta\rho, \delta T)
\end{aligned}
$$

- Therefore, the Jacobian of the resistive MHD model has the following coupling structure:

$$
J\delta\vec{x} = \begin{bmatrix} D_\rho & 0 & 0 & U_{v\rho} \\ 0 & D_T & 0 & U_{vT} \\ 0 & 0 & D_B & U_{vB} \\ L_{\rho v} & L_{Tv} & L_{Bv} & D_v \end{bmatrix} \begin{pmatrix} \delta\rho \\ \delta T \\ \delta\vec{B} \\ \delta\vec{v} \end{pmatrix}
$$

- Diagonal blocks contain advection-diffusion contributions, and are "easy" to invert using MG techniques. Off diagonal blocks L and U contain all hyperbolic couplings.

Luis Chacon, chacon@lanl.gov

PARABOLIZATION: Schur-complement formulation

- We consider the block structure:

$$J\delta\vec{x} = \begin{bmatrix} M & U \\ L & D_v \end{bmatrix} \begin{pmatrix} \delta\vec{y} \\ \delta\vec{v} \end{pmatrix} \; ; \; \delta\vec{y} = \begin{pmatrix} \delta\rho \\ \delta T \\ \delta\vec{B} \end{pmatrix} \; ; \; M = \begin{pmatrix} D_\rho & 0 & 0 \\ 0 & D_T & 0 \\ 0 & 0 & D_B \end{pmatrix}$$

- M is "easy" to invert (advection-diffusion, not very stiff, MG-friendly).

Schur complement analysis of 2x2 block J yields:

$$\begin{bmatrix} M & U \\ L & D_v \end{bmatrix}^{-1} = \begin{bmatrix} I & 0 \\ -LM^{-1} & I \end{bmatrix} \begin{bmatrix} M^{-1} & 0 \\ 0 & P_{Schur}^{-1} \end{bmatrix} \begin{bmatrix} I & -M^{-1}U \\ 0 & I \end{bmatrix},$$

$$P_{Schur} = D_v - LM^{-1}U \; .$$

- EXACT Jacobian inverse only requires M^{-1} and P_{Schur}^{-1}.
- Schur complement formulation is fundamentally unchanged in extended MHD!

Luis Chacon, chacon@lanl.gov

Physics-based preconditioner (PBP)

- The Schur complement analysis translates into the following 3-step EXACT inversion algorithm:

$$\begin{aligned}
\text{Predictor} \quad &: \quad \delta\vec{y}^* = -M^{-1}G_y \\
\text{Velocity update} \quad &: \quad \delta\vec{v} = P_{Schur}^{-1}[-G_v - L\delta\vec{y}^*],\ P_{Schur} = D_v - LM^{-1}U \\
\text{Corrector} \quad &: \quad \delta\vec{y} = \delta\vec{y}^* - M^{-1}U\delta\vec{v}
\end{aligned}$$

- MG treatment of P_{Schur} is impractical due to M^{-1}.
  - Small-flow limit: $v \ll v_A \Rightarrow$ $M^{-1} \approx \Delta t$
  - We have developed extensions for arbitrary flows

Luis Chacon, chacon@lanl.gov

PBP: small-flow limit

- Small flow approximation: $M^{-1} \approx \Delta t$ in steps 2 & 3 of Schur algorithm:

$$
\begin{aligned}
\delta\vec{y}^* &= -M^{-1}\, G_y \\
\delta\vec{v} &\approx P_{SI}^{-1}\left[-G_v - L\delta\vec{y}^*\right] \;;\; P_{SI} = D_v - \Delta t L U \\
\delta\vec{y} &\approx \delta\vec{y}^* - \Delta t U \delta\vec{v}
\end{aligned}
$$

where:

$$
\boxed{P_{SI} = \rho^n \left[\overleftrightarrow{I}/\Delta t + \theta(\vec{v}_0 \cdot \nabla \overleftrightarrow{I} + \overleftrightarrow{I} \cdot \nabla \vec{v}_0 - \nu^n \nabla^2 \overleftrightarrow{I})\right] + \Delta t \theta^2 W(\vec{B}_0, p_0)}
$$

$$
W(\vec{B}_0, p_0) = \vec{B}_0 \times \nabla \times \nabla \times [\overleftrightarrow{I} \times \vec{B}_0] - \vec{j}_0 \times \nabla \times [\overleftrightarrow{I} \times \vec{B}_0] - \nabla[\overleftrightarrow{I} \cdot \nabla p_0 + \gamma p_0 \nabla \cdot \overleftrightarrow{I}]
$$

- P_{SI} is block diagonally dominant by construction!
- We employ multigrid methods (MG) to approximately invert P_{SI} and M: 1 V(4,4) cycle

Luis Chacon, chacon@lanl.gov

PBP: 2D serial performance (tearing mode)

Δt convergence study (128x128)

Δt	GMRES/Δt	CPU_{exp}/CPU	$\Delta t/\Delta t_{CFL}$
0.5	**8.0**	8.0	380
0.75	**9.5**	10.0	570
1.0	**11.2**	12.7	760
1.5	**14.6**	14.6	1140

Grid convergence study ($\Delta t = 1200\Delta t_{CFL}$)

N	GMRES/Δt	CPU_{exp}/CPU	$\Delta t/\Delta t_{CFL}$
32x32	14	2.43	159
64x64	11.8	5.8	322
128x128	11.2	13.3	667
256x256	11.4	28.5	1429

$CPU \sim \mathcal{O}(N)$ OPTIMAL SCALING!

Luis Chacon, chacon@lanl.gov

PBP: 3D serial performance (island coalescence)

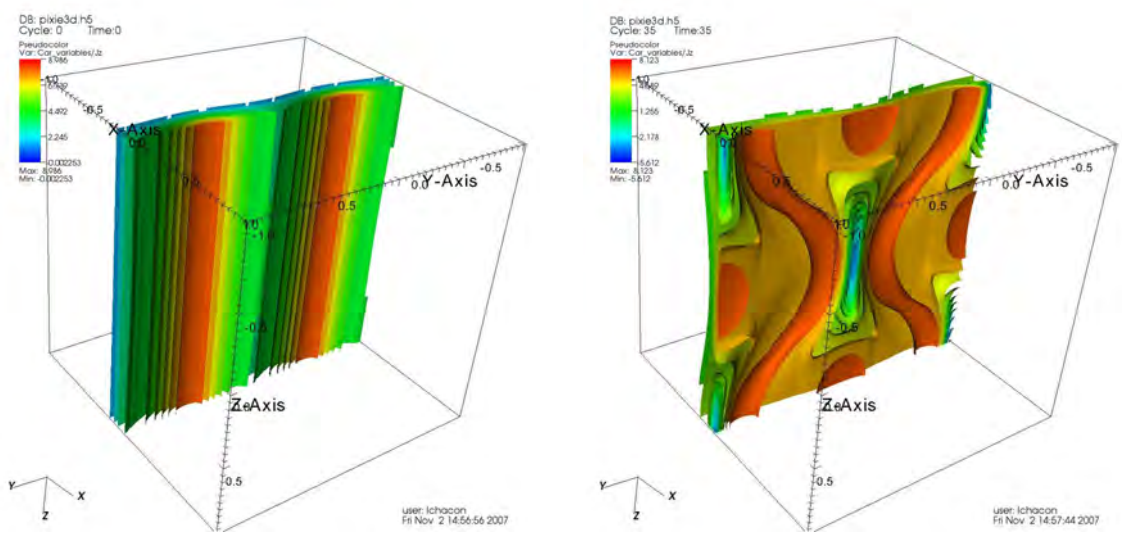

10 time steps, $\Delta t = 0.1$, V(3,3) cycles, mg_tol=1e-2

Grid	GMRES/Δt	CPU
16^3	5.5	81
32^3	7.9	1176
64^3	7.0	11135

Luis Chacon, chacon@lanl.gov

PBP: 3D parallel performance (island coalescence)
(16^3 grid points per processor; old result – 2008)

$$\Delta t = 0.1 \gg \Delta t_{CFL}$$

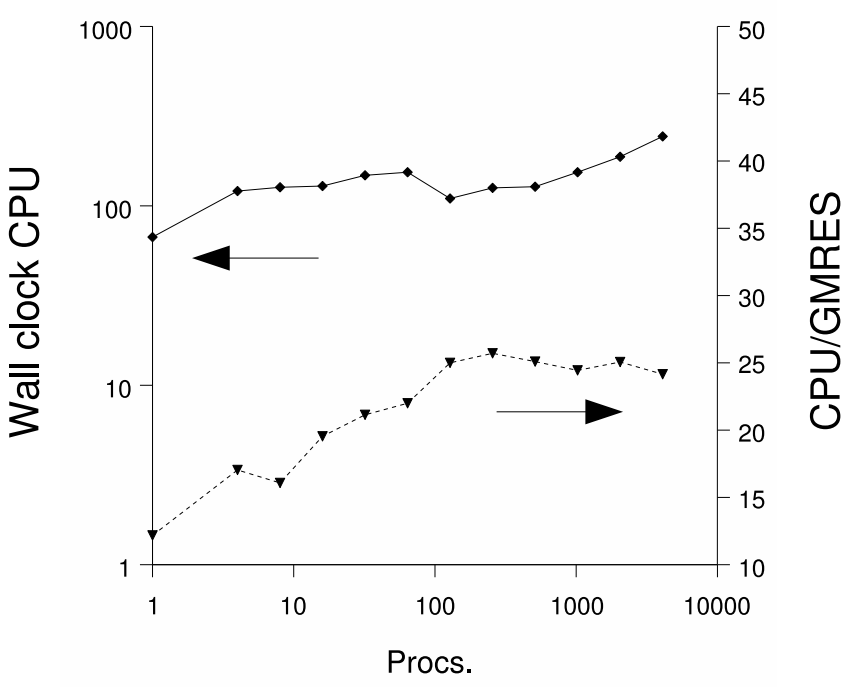

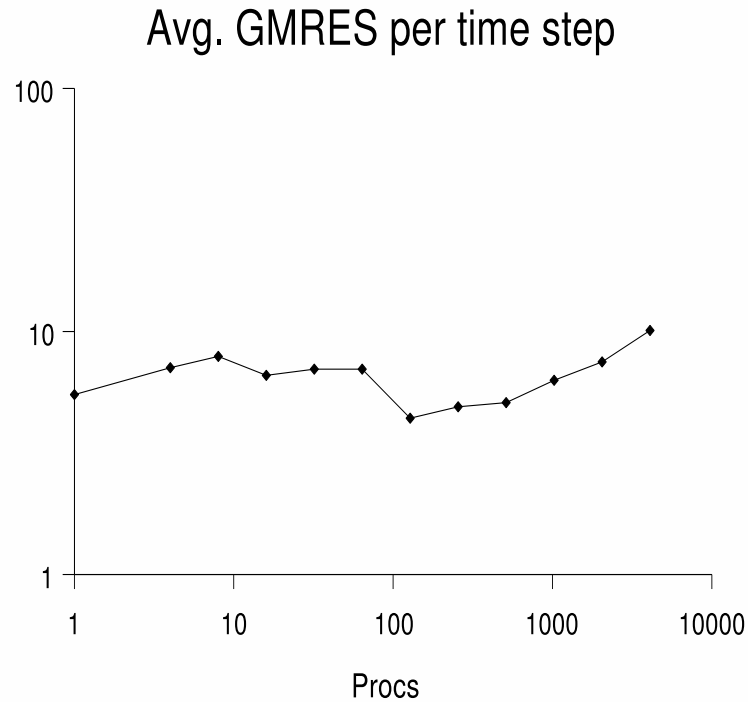

Los Alamos NATIONAL LABORATORY EST. 1943

Luis Chacon, chacon@lanl.gov

Verification: Solov'ev Equilibria

($\kappa = 1$, n=2, $64 \times 64 \times 64$)[13]

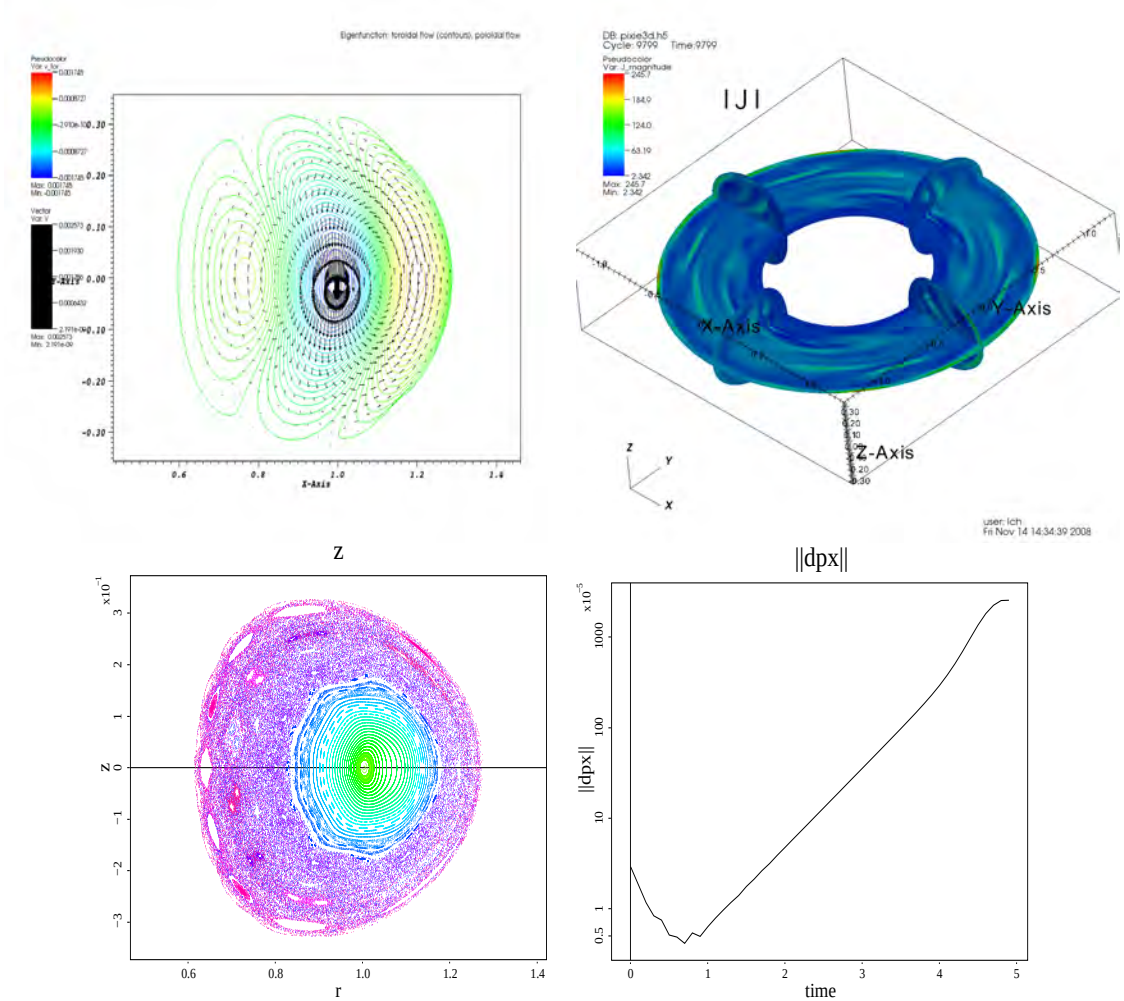

$\gamma_{PIXIE3D} = 2.01$ (vs. 2.196 in Schnack et al. in our units)

[13] See e.g. Schnack et al., JCP 140 (1998) and refs. therein

Luis Chacon, chacon@lanl.gov

Application: Sawteeth mitigation by boundary magnetic perturbations[14]

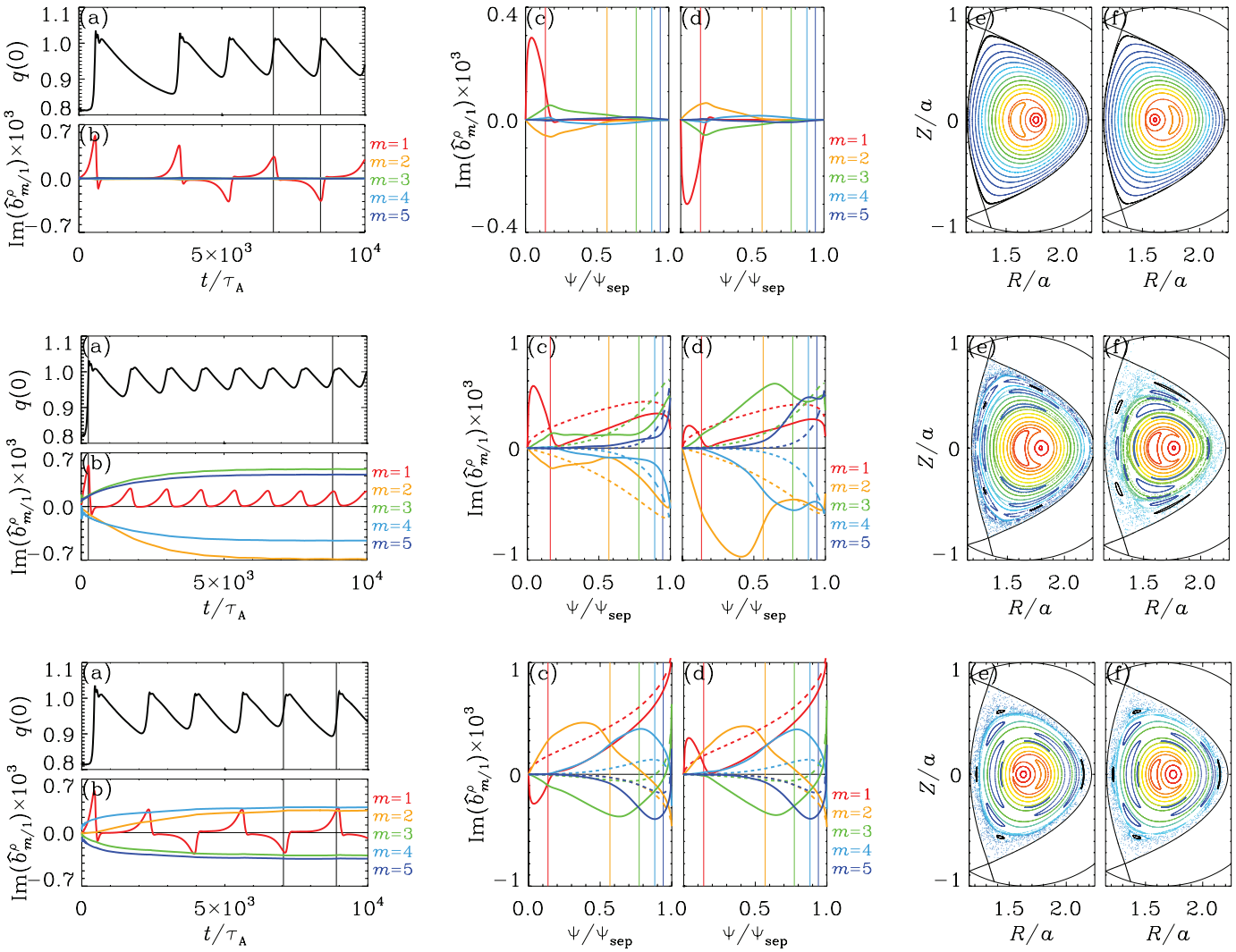

[14] Bonfiglio et al., PPCF, 59 (2017)

Luis Chacon, chacon@lanl.gov

Physics applications of PIXIE3D resistive MHD solver

Resistive PIXIE3D has been applied to reconnection and MFE (RFP, tokamak, stellarator)

1. A. Stanier, W. Daughton, Andrei N. Simakov, L. Chacón, A. Le, H. Karimabadi, Jonathan Ng, and A. Bhattacharjee, "The role of guide field on magnetic reconnection during island coalescence," Phys. Plasmas, 24, 022124 (2017)
2. D. Bonfiglio, M. Veranda, S. Cappello, L. Chacón, and D. F. Escande, "Sawtooth mitigation in 3D MHD tokamak modelling with applied magnetic perturbations," Plasma Physics and Controlled Fusion, 59, 014032 (2017)
3. D. Bonfiglio, M. Veranda, S. Cappello, D. F. Escande, L. Chacón, "Helical self-organization in 3D MHD modelling of fusion plasmas," Plasma Phys. Controlled Fusion, 57, 044001 (2015)
4. L. Piron, P. Piovesan, F. Auriemma, D. Bonfiglio, L. Carraro, L. Chacón, L. Marrelli, M. Valisa, M. Veranda, B. Zaniol, M. Zuin, "3D magnetic fields and plasma rotation in RFX-mod tokamak plasmas," Nucl. Fusion, 53, 113022 (2013)
5. D. Bonfiglio, M. Veranda, S. Cappello, D. F. Escande, and L. Chacón, "Experimental-like helical self-organization in reversed-field pinch modeling," Phys. Rev. Lett., 111 (8), 085002 (2013)
6. P. Piovesan et al., "RFX-mod: a multi-configuration fusion facility for 3D physics studies," Phys. Plasmas, 20, 056112 (2013)
7. M. Veranda, D. Bonfiglio, S. Cappello, L. Chacón, D. F. Escande, "Impact of helical boundary conditions on nonlinear 3D MHD simulations of the reversed-field pinch," Plasma Phys. Controlled Fusion, 55, 074015 (2013)
8. S. Cappello, D. Bonfiglio, D.F. Escande, S.C. Guo, I. Predebon, F. Sattin, M. Veranda, P. Zanca, C. Angioni, L. Chacón, J.Q. Dong, X. Garbet, and S.F. Liu, "Equilibrium and transport for quasi-helical reversed field pinches," Nucl. Fusion 51, 103012 (2011)
9. D. Bonfiglio, L. Chacón, S. Cappello, "Nonlinear 3D verification of the SpeCyl and PIXIE3D MHD codes for fusion plasmas," Phys. Plasmas, 17, 082501 (2010)

3D *extended* MHD implicit solver

L. Chacon, in preparation

Los Alamos NATIONAL LABORATORY EST. 1943

Luis Chacon, chacon@lanl.gov

Extended (two-fluid, Hall) MHD model equations
(vector potential form)

$$\frac{\partial \rho}{\partial t} + \nabla \cdot (\rho \vec{v}) = 0,$$

$$\boxed{\frac{\partial \vec{A}}{\partial t} + \vec{E} = -\nabla \phi} \quad ; \quad \vec{B} = \nabla \times \vec{A}\,, \boxed{\phi = -\frac{d_e^2}{d_i}\frac{\mathbf{v}_e^2}{2}} \text{(Gauge)}$$

$$\frac{\partial(\rho\vec{v})}{\partial t} + \nabla \cdot \left[\rho\vec{v}\vec{v} - \vec{B}\vec{B} + \overleftrightarrow{\Pi}_i + \overleftrightarrow{I}(p + \frac{B^2}{2})\right] = 0,$$

$$\frac{\partial p_e}{\partial t} + \nabla \cdot (\vec{v} p_e) + (\gamma - 1) p_e \nabla \cdot \vec{v} = (\gamma - 1)(S - \nabla \cdot \vec{q}).$$

$$\vec{v} = \frac{m_i \vec{v}_i + m_e \vec{v}_e}{m_i + m_e} \approx \vec{v}_i \ ; \ \vec{v}_e = \vec{v}_i - d_i \frac{\vec{j}}{\rho}$$

$$\text{Ohm's Law}: \vec{E} = -\vec{v} \times \vec{B} + \eta \vec{j} - \frac{d_i}{\rho}(\vec{j} \times \vec{B} - \nabla p_e - \nabla \cdot \overleftrightarrow{\Pi}_e) - \frac{d_e^2}{d_i}\frac{d\vec{v}_e}{dt}$$

Luis Chacon, chacon@lanl.gov

Extended MHD Jacobian block structure

$$\vec{E} = -\vec{v}\times\vec{B} + \eta\vec{j} - \frac{d_i}{\rho}(\vec{j}\times\vec{B} - \nabla p_e - \nabla\cdot\overleftrightarrow{\Pi}_e) - \frac{d_e^2}{d_i}\frac{d\vec{v}_e}{dt} \;;\; \overleftrightarrow{\Pi}_e = -\rho\nu_e\nabla\vec{v}_e \approx \rho d_i\nu_e\nabla(\frac{\vec{j}}{\rho})$$

- Linearized induction equation $\delta\vec{B} = -\nabla\times\delta\vec{E}$ has the following couplings:

$$\delta\mathbf{A} \quad = \quad L_B(\delta\mathbf{A}, \delta\mathbf{v}, \delta\rho, \delta p_e)$$

- Jacobian coupling structure:

$$J\delta\mathbf{x} = \begin{bmatrix} D_\rho & 0 & 0 & U_{\rho\mathbf{v}} \\ \boxed{L_{p\rho}} & D_p & \boxed{U_{p\mathbf{A}}} & U_{p\mathbf{v}} \\ \boxed{L_{\mathbf{A}\rho}} & \boxed{L_{\mathbf{A}p}} & D_{\mathbf{EMHD}} & U_{\mathbf{vA}} \\ L_{\mathbf{v}\rho} & L_{\mathbf{v}p} & L_{\mathbf{vA}} & D_{\mathbf{v}} \end{bmatrix} \begin{pmatrix} \delta\rho \\ \delta p_e \\ \delta\vec{A} \\ \delta\vec{v} \end{pmatrix}$$

- We have added off-diagonal couplings and stiff time scales to block M, which in principle complicates block-factorization approach.
- However, all except $D_{\mathbf{EMHD}}$ are trivial (disappear in homogeneous plasma); $D_{\mathbf{EMHD}}$ contains whistler wave.

Luis Chacon, chacon@lanl.gov

Extended MHD preconditioner

- Consider approximation (neglect Joule heating source):

$$J \approx P = \begin{bmatrix} M & U \\ L & D_v \end{bmatrix} \; ; \; M = \begin{pmatrix} D_\rho & 0 & 0 \\ \boxed{L_{p\rho}} & D_p & 0 \\ \boxed{L_{\mathbf{A}\rho}} & \boxed{L_{\mathbf{A}p}} & \boxed{D_{\mathbf{EMHD}}} \end{pmatrix}$$

- Use same block factorization approach:

$$\begin{aligned} \delta\vec{y}^* &= -M^{-1} G_y \\ \delta\vec{v} &\approx P_{SI}^{-1} \left[-G_v - L\delta\vec{y}^* \right] \; ; \; P_{SI} = D_v - \Delta t L U \\ \delta\vec{y} &\approx \delta\vec{y}^* - \Delta t U \delta\vec{v} \end{aligned}$$

- M block now contains whistler time scales.
  - First M^{-1} solve (via $D_{\mathbf{EMHD}}$ inversion) addresses electron stiff time scales by operator splitting.
  - Subsequent solves address ionic timescales, and approximation $M^{-1} \approx \Delta t$ is sufficient.

Luis Chacon, chacon@lanl.gov

Inversion of EMHD block ($D_{\mathbf{EMHD}}$)

- $D_{\mathbf{A}}$ block contains EMHD electron physics:

$$
\begin{aligned}
D_{\mathbf{EMHD}}\delta\mathbf{A} &= \frac{\delta\mathbf{A}^*}{\Delta t} - \theta\left(\mathbf{v}_{e,0}\times\nabla\times\delta\mathbf{A}^* - d_i\underbrace{\frac{\nabla\times\nabla\times\delta\mathbf{A}}{\rho_0}\times\mathbf{B_0}}_{\text{Whistler}} - \eta\nabla\times\nabla\times\delta\mathbf{A} + \underbrace{\nabla\cdot\left[\rho_0 d_i\nu_e\nabla\left(\frac{\nabla\times\nabla\times\delta\mathbf{A}}{\rho_0}\right)\right]}_{\text{Hyperresistivity}}\right)\\
\delta\mathbf{A}^* &= \delta\mathbf{A} + \frac{d_e^2}{\rho_0}\nabla\times\nabla\times\delta\mathbf{A}
\end{aligned}
$$

- Hyperresistivity is a 4th order operator on $\delta\mathbf{A}$ of mixed character.
  - We do NOT use Coulomb gauge $\nabla\cdot\mathbf{A}=0$, so $\nabla\times\nabla\times$ cannot be replaced by $-\nabla^2$ in general.
- It is needed to provide a dissipation length scale to dispersive waves $\omega\sim k_{\|}k$.
- We have implemented this in MG by considering 2 second-order vector systems:

$$
\begin{aligned}
\frac{1}{\Delta t}\left(\delta\mathbf{A}+d_e^2\frac{\delta\mathbf{j}}{\rho_0}\right) - \theta\left(\mathbf{v}_{e,0}\times\nabla\times\left(\delta\mathbf{A}+d_e^2\frac{\delta\mathbf{j}}{\rho_0}\right) - d_i\frac{\delta\mathbf{j}}{\rho_0}\times\mathbf{B_0} - \eta\delta\mathbf{j} + \nabla\cdot\left[\rho_0 d_i\nu_e\nabla\left(\frac{\delta\mathbf{j}}{\rho_0}\right)\right]\right) &= \text{rhs}\\
\delta\mathbf{j} - \nabla\times\nabla\times\delta\mathbf{A} &= 0
\end{aligned}
$$

  - Well defined set of boundary conditions for $\delta\mathbf{j}$ (critical; not the case for $\mathbf{B}$ formulation)
  - Block smoothing in MG (critical)
  - Used $\nabla\times\nabla\times\Rightarrow-\nabla^2$ in block diagonal inverse for smoothing step (critical)

Luis Chacon, chacon@lanl.gov

2D nonlinear verification: GEM challenge
PIXIE3D vs. HiFi (V. Lukin, A. Glasser)

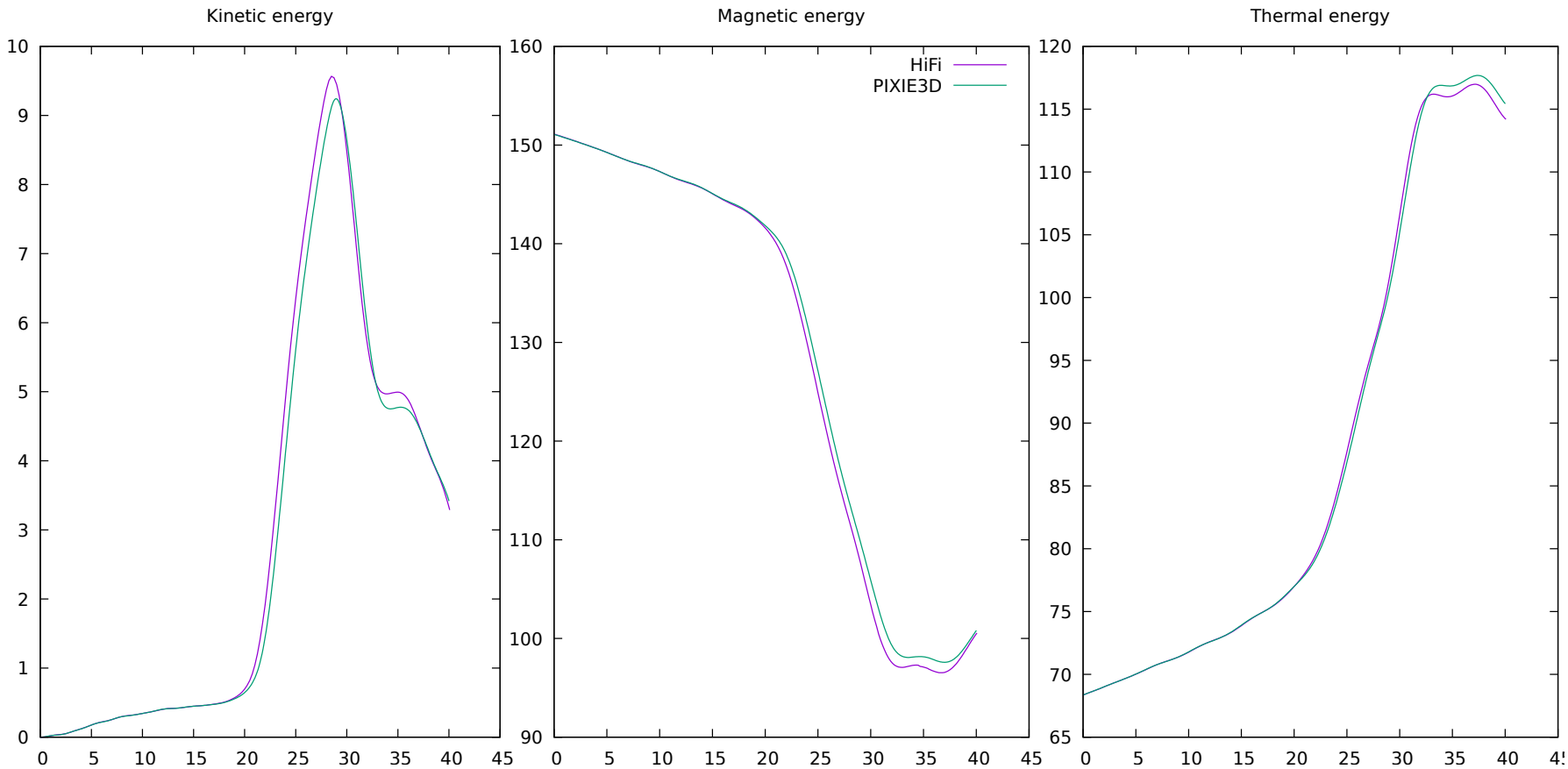

Luis Chacon, chacon@lanl.gov

Extended MHD performance results (GEM challenge)

$$d_i/L_x = 1/12.8,\ \eta = \nu_i = \kappa = 5 \times 10^{-4}$$

100 time steps, $\Delta t = 0.01$, 1 V(4,4) MG cycle

np	mesh	ν_e	$\frac{\Delta t}{\Delta t_{exp}}$	GMRES/Δt	Newton/Δt	WCT(s)	WCT/PC
1	32×32	10^{-4}	1.0	2	2	174	43.5
4	64×64	2.5×10^{-5}	2.1	2	2	214	53.5
16	128×128	6.3×10^{-6}	8.2	2	2	298	74.5
64	256×256	1.6×10^{-6}	170	7	3.8	1030	95.4
256	512×512	3.9×10^{-7}	130	3.2	2.4	648	115.7
1024	1024×1024	9.8×10^{-8}	520	2.9	2.4	961	181.3
4096	2048×2048	2.4×10^{-8}	2100	4.1	2.7	1350	198.5

- Grid-bound ν_e to avoid unnecessary 4th-order operator stiffness: $\nu_e \propto \frac{d_i v_A k_{\|}}{k^3}$
- Implicit algorithm WCT increases by 8 from 1 to 4096 cores; explicit algorithm WCT would increase by 4096 from quadratic CFL!

Luis Chacon, chacon@lanl.gov

Conclusions

- Developed a scalable, multilevel-based, fully implicit NK-MG solver for the 2D low-β and 3D primitive-variable extended MHD models.

Key algorithmic breakthrough: $\mathrm{PARABOLIZATION} + \mathrm{MG}$.

- Demonstrated excellent algorithmic performance under grid refinement and with time step.
- Demonstrated excellent parallel performance.
- Used the 2D low-β tool to explore fast magnetic reconnection physics with large guide fields:
  - Fast reconnection is characterized by being independent of both dissipation and system size
  - We have demonstrated that fast reconnection is ubiquitous in all extended low-β regimes ($d_e, \rho_s \neq 0$) (a new result)
  - We have found excellent agreement between fluid and kinetic simulations, qualitatively and quantitatively (a new result)
- The 3D resistive MHD tool has been used to model RFP, Tokamaks, and currently being adapted for stellarators
- The 3D extended MHD tool has been used mainly in magnetic reconnection studies, and is currently being extended to toroidal geometry.

Luis Chacon, chacon@lanl.gov